

Supporting Information

# **Functionalized-Ferroelectric-Coatings-Driven Enhanced Biom mineralization and Protein-Conformation on Metallic Implants**

*Sebastian Zlotnik <sup>#a</sup>, Marisa Maltez-da Costa <sup>a</sup>, Nathalie Barroca <sup>a</sup>, María J. Hortigüela <sup>b</sup>, Manoj Kumar Singh <sup>b</sup>, Maria Helena V. Fernandes <sup>a</sup>, Paula Maria Vilarinho <sup>\*a</sup>*

<sup>a</sup> Department of Materials and Ceramic Engineering, CICECO – Aveiro Institute of Materials, University of Aveiro, 3810-193 Aveiro, Portugal

<sup>b</sup> Center for Mechanical Technology and Automation (TEMA), Department of Mechanical Engineering, University of Aveiro, 3810-193 Aveiro, Portugal

Emails: [sebastian.zlotnik@itme.edu.pl](mailto:sebastian.zlotnik@itme.edu.pl), [marisamaltez@ua.pt](mailto:marisamaltez@ua.pt), [nbarroca@ua.pt](mailto:nbarroca@ua.pt), [mhortiguela@ua.pt](mailto:mhortiguela@ua.pt), [mksingh@ua.pt](mailto:mksingh@ua.pt), [helena.fernandes@ua.pt](mailto:helena.fernandes@ua.pt), [paula.vilarinho@ua.pt](mailto:paula.vilarinho@ua.pt)

<sup>#</sup> Present address: Institute of Electronic Materials Technology, Wolczynska 133, 01-919 Warsaw, Poland

\* Corresponding author: [paula.vilarinho@ua.pt](mailto:paula.vilarinho@ua.pt)

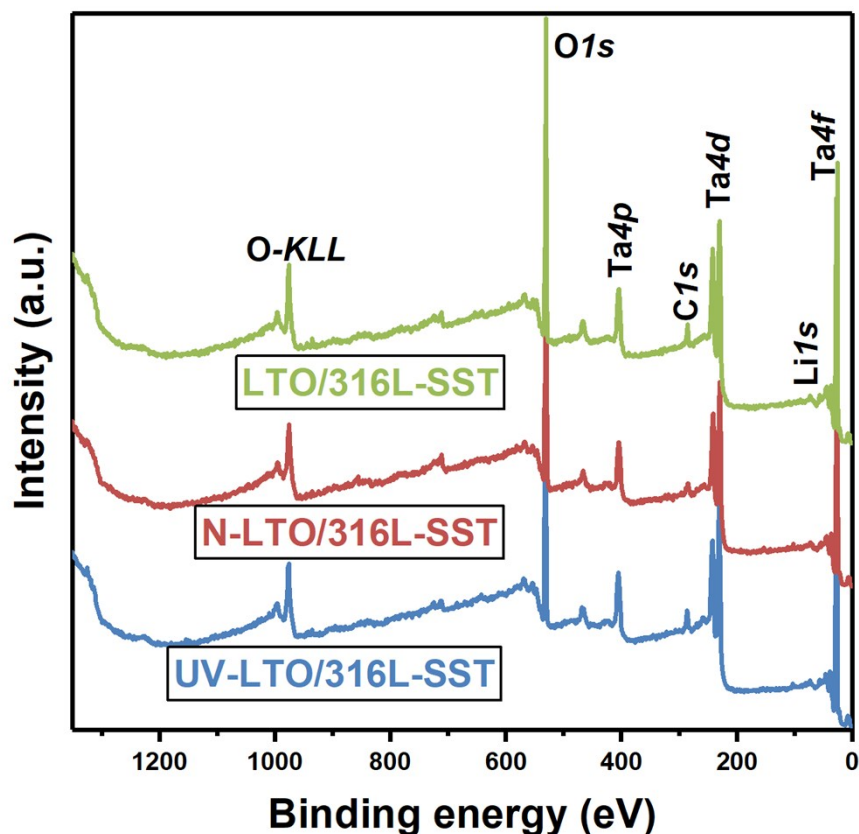


**Figure S1.** General X-ray photoelectron spectroscopy (XPS) scans of as-coated LTO and functionalized LTO onto 316L-SST.

The presence of lithium, tantalum, oxygen and carbon is evident in the general XPS spectra. The Ta 4f signal is composed of two peaks (not magnified here), Ta 4f<sub>7/2</sub> and Ta 4f<sub>5/2</sub> spin orbital splitting at ~26 eV and ~28 eV, respectively. The energy position of these peaks is characteristic of the binding energy of Ta<sup>5+</sup>, thus it is a proof of the presence of tantalum pentoxide, Ta<sub>2</sub>O<sub>5</sub><sup>1</sup>. The Ta 4f spectrum shows also a tail with negligible intensity at ~22 eV that can be assigned to metallic Ta<sup>1,2</sup>.

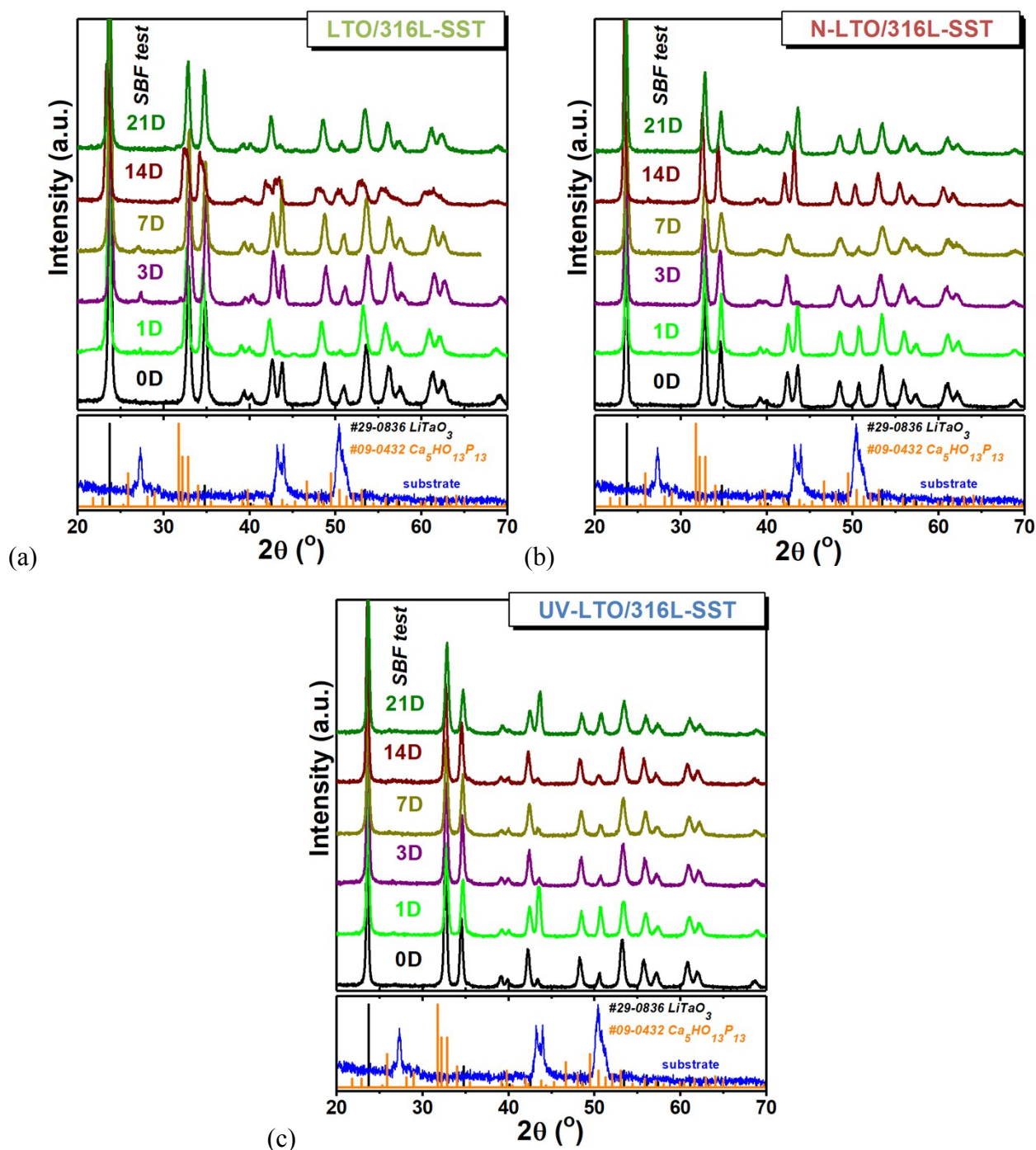


**Figure S2.** XRD patterns of LTO coatings: (a) as-prepared, (b) polarized and (c) UV-irradiated, soaked in SBF solution for 1, 3, 7, 14 and 21 days. Diffraction lines of  $\text{LiTaO}_3$  (JCPDS-PDF #29-0836), hydroxyapatite (JCPDS-PDF #09-0432), and diffractogram of bare 316L-SST are enclosed as well in the bottom frame. There are no appreciable variations in the XRD patterns and no indication of hydroxyapatite (JCPDS-PDF #09-0432) formation.

Figure S2 shows the X-ray diffraction patterns of the three sets of examined coatings: i) LTO/316L-SST (Figure S2 (a)), ii) N-LTO/316L-SST (Figure S2 (b)), and iii) UV-LTO/316L-

SST (Figure S2 (c)); for comparison additional reference patterns of the substrate,  $\text{LiTaO}_3$  (JCPDS-PDF file #29-0836) and apatite (JCPDS-PDF file #09-0432) are included at the bottom of the figure. All the coatings exhibit monophasic patterns composed of crystalline LTO (matching JCPDS-PDF file #29-0836) and do not show evidences of crystalline or amorphous (identified as broad halos background near the main diffraction lines) calcium phosphate phases when compared to the standards (0D coatings). A degree of uncertainty may be associated with these observations resulting from the equipment detection limit ( $>3$  vol%), the low degree of crystallinity of the newly formed phases when compared with the underneath layers (LTO and 316L-SST) both with a high degree of crystallinity and the possible overlapping of the diffraction lines of LTO and apatite phases, that may interfere with phase identification.

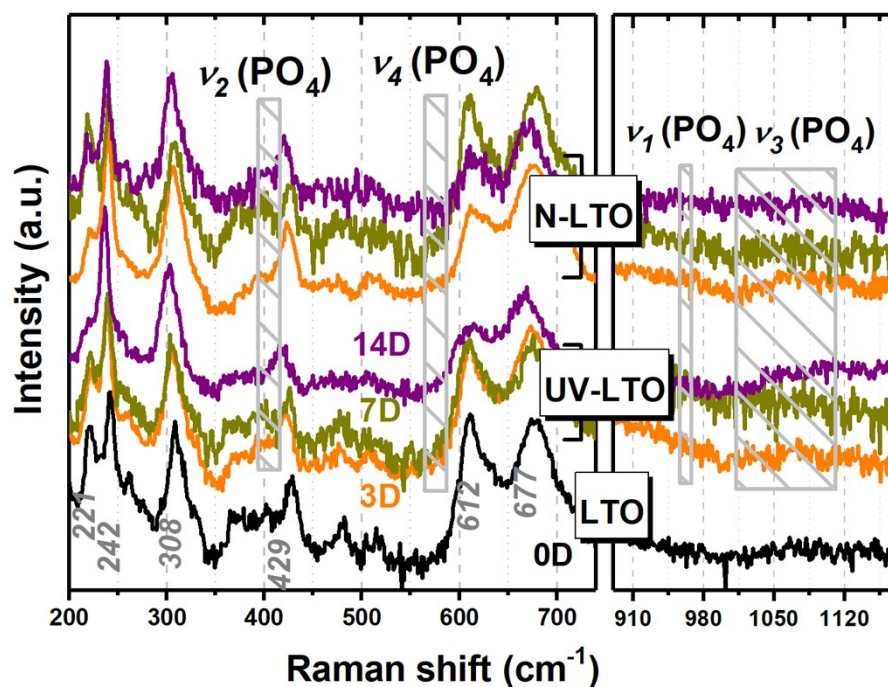


**Figure S3.** Raman spectra of polarized and UV-irradiated LTO films immersed in SBF solution for 3, 7 and 14 days. Vibration positions of  $\text{PO}_4^{3-}$  group (bending,  $\nu_2$  and  $\nu_4$ , and stretching,  $\nu_1$  and  $\nu_3$ , modes) are marked, but only multiple peaks for both  $A_1$  and  $E$  modes because of the polycrystalline character of thin film are detected.

Raman spectra of as-deposited as well as polarized and UV-treated LTO coatings incubated in SBF solution for 3, 7 and 14 days are shown in Figure S3. Once again the graph is separated in two regions: i) 200 - 750  $\text{cm}^{-1}$  and ii) 900 - 1160  $\text{cm}^{-1}$ . The spectra are composed of many peaks, some of them are sharp and clear and others broad mostly due to superposition of more than one phonon mode. The spectrum of LTO/316L-SST (bottom plot, 0D) is composed of peaks for both  $A_1$  and  $E$  modes (transverse and longitudinal) due to the polycrystalline character of these coatings. It has been reported that the fundamental phonon mode positions in Raman spectrum of  $\text{LiTaO}_3$  are located at 74, 140, 206, 251, 316, 383, 462, 596, and 662  $\text{cm}^{-1}$  for  $E(\text{TO})$ , at 80, 163, 248, 278, 318, 452, 474, 648, and 870  $\text{cm}^{-1}$  for  $E(\text{LO})$ , at 201, 253, 356, and 600  $\text{cm}^{-1}$  for  $A_1(\text{TO})$ , and at 245, 347, 401, and 864  $\text{cm}^{-1}$  for  $A_1(\text{LO})$ <sup>3</sup>. Many of the minor peaks that cannot be assigned to any of the listed modes might be attributed to the strain at the substrate / coating interface or to lattice defects as oxygen vacancies and slight non-stoichiometry<sup>4</sup>.

## References:

- 1 E. Atanassova, G. Tyuliev, A. Paskaleva, D. Spassov and K. Kostov, *Appl. Surf. Sci.*, 2004, **225**, 86–99.
- 2 J. Liu, J. Liu and Z. Li, *J. Solid State Chem.*, 2013, **198**, 192–196.
- 3 A. S. Barker, A. A. Ballman and J. A. Ditzenberger, *Phys. Rev. B*, 1970, **2**, 4233–4239.
- 4 S. Satapathy, S. Kumar, B. N. Raja Sekhar, V. G. Sathe and P. K. Gupta, *J. Appl. Phys.*, 2008, **104**, 033542.